separations

MDPI

Article

Selective Recovery of Gold Using Two Sea Algae (*Ulva lactuca* and *Ulva pertusa*) with or Without Concentrated Sulfuric Acid Treatment

Jhapindra Adhikari [1], Gehui Pang [1,2], Shintaro Morisada [1], Hidetaka Kawakita [1], Keisuke Ohto [1,*], Mikihide Demura [3] and Kazuya Urata [4]

[1] Department of Chemistry and Applied Chemistry, Faculty of Science and Engineering, Saga University, 1-Honjo, Saga 840-8502, Japan
[2] College of Light Industry, Liaoning University, Shenyang 110036, China
[3] Faculty of Agriculture, Saga University, 1-Honjo, Saga 840-8502, Japan
[4] Institute of Ocean Energy, Saga University, Imari Satellite, 1-48 Hirao, Saga 849-4256, Japan
* Correspondence: ohtok@cc.saga-u.ac.jp

Abstract

Four algal adsorbents were prepared from two types of green sea algae (*Ulva lactuca* and *Ulva pertusa*), either by treatment with concentrated sulfuric acid or without treatment. A comparative study of Au(III) adsorption in an HCl medium was performed. While both untreated adsorbents showed good performance at low HCl concentrations, the treated adsorbents achieved quantitative adsorption and high selectivity for Au(III) across a broad range of HCl concentrations. The adsorption of Au(III) onto the algal biomass adsorbents followed the typical Langmuir monolayer adsorption model. At an HCl concentration of 0.010 M, the maximum adsorption capacities were 1.14, 0.86, 6.57, and 6.28 mol kg^{-1} for **DUL**, **DUP**, **TUL**, and **TUP**, respectively. A kinetic study conducted at different temperatures was consistent with the pseudo-first-order kinetic model and enabled estimation of the activation energy of the adsorption reaction. Structural changes before and after treatment were analyzed using FT-IR spectroscopy. Confirmation of Au(III) adsorption and its subsequent reduction to the elemental state was achieved through XRD and SEM/EDX analyses as well as digital imaging of the Au-loaded adsorbents. Finally, the adsorbed and reduced Au was successfully desorbed using an acidic thiourea solution.

Keywords: gold recovery; adsorption; reduction; algal biosorbents; green waste; sulfuric acid treatment

Academic Editor: Zhiqian Jia

Received: 30 March 2026
Revised: 24 April 2026
Accepted: 27 April 2026
Published: 30 April 2026

1. Introduction

Gold (Au) has been one of the most valuable metals since ancient times and is used in a wide range of applications, including jewelry, electronic and medical devices, and industrial catalysts, due to its high electrical conductivity and corrosion resistance [1–3]. The price of Au has increased, likely because of the rapid growth in demand from high-tech industries and the declining availability of primary metal resources. Recently, interest in extracting Au from secondary resources has surged, as its concentration in such materials (e.g., electronic and catalytic wastes, ~200 g ton^{-1}) is significantly higher than in natural ores (5–30 g ton^{-1}) [4–7]. It is estimated that the amount of Au recovered from one ton of computer waste exceeds that obtained from 17 tons of mined ore [8]. Moreover, recovering Au from secondary resources not only reduces mining costs but also supports the sustainable use of non-renewable mineral resources and helps maintain the supply–demand

balance [9,10]. Mobile and computer devices account for approximately 4% of total Au consumption [11]. The global production of waste electrical and electronic equipment (WEEE) reached 53.6 million tons (Mt) in 2019 and is projected to increase to 74.7 Mt by 2030 [12]. Although Au recovery from secondary resources is economically attractive, less than 20% of e-waste is currently recycled, mainly due to the lack of efficient technologies [13].

Conventional techniques such as cementation, precipitation, ion exchange, and solvent extraction, which are used for recovering precious metals (PMs), are neither economically feasible nor environmentally friendly [14]. Solvent extraction is a lengthy process due to the need for multiple extraction steps, and the use of flammable and hazardous organic solvents contributes to environmental pollution [11,15]. Precipitation is relatively inexpensive; however, it requires large volumes of precipitants and generates significant waste [16]. Ion exchange technologies are simple, cost-effective, and environmentally friendly, but they require longer separation cycles [17,18]. Chemical methods involving cyanidation and thiourea leaching for Au extraction pose serious risks to both the environment and human health. Techniques based on the use of activated carbon are more commonly employed for Au extraction because of its high surface area and porous structure; however, they have notable limitations, including low extraction capacity, poor selectivity, and high energy and chemical requirements for regeneration [13,19,20]. Consequently, there is a need to develop innovative techniques for recovering Au ions from aqueous solutions that are environmentally friendly and pose fewer risks to human health [21].

As an alternative to conventional techniques, biodegradable adsorbents show great promise for recovering PMs or removing hazardous metals from aqueous environments due to their effectiveness, availability, versatility, and reliability across a wide range of metal ion concentrations [11,22]. The binding of metal ions in solution to chemical sites on the biomass adsorbent is a passive and metabolically independent process that occurs over a broad range of pH values and temperatures without generating secondary wastes [23,24]. The potential of biosorbents for recovering precious metals has increased with the growing emphasis on environmental sustainability and the circular economy [25,26]. A review article indicated that among valuable metals, the greatest focus (34%) has been on the biosorption of Au [8]. A wide variety of biomaterials, including fruit peels [5,6,10,20], chitosan [16], eggshell membranes [27], plant leaves [28], sheep wool [29], chicken feathers [30], and microalgae [31,32], have been used as adsorbents, with or without chemical modification, for Au(III) adsorption. Biosorbents not only reduce operational complexity but also serve as effective alternatives to commonly used commercial materials such as activated carbon and ion-exchange resins.

Algae are responsible for approximately 90% of global photosynthesis, and their cell wall polymers account for about half of all non-aqueous biomass. The use of marine algae as biosorbents for metal recovery is increasing due to their high biopolymer content, including polysaccharides, proteins, and lipids [33,34]. Furthermore, their high metal binding capacity, low cost, regeneration efficiency, high surface-to-volume ratio, and macroscopic structure provide significant advantages as adsorbents [25,35]. The use of algal biomass for the recovery of Au(III) is particularly beneficial because it is environmentally friendly and readily available in large quantities at low cost throughout the year [36]. Cell wall components rich in functional groups such as hydroxyl (-OH), amine (-NH_2), amide (-$CONH_2$), and carboxy (-COOH) groups serve as the most efficient sites for Au(III) adsorption by green algae [37,38]. Algae are also a major source of cellulose, producing approximately 10^{11}–10^{12} tons annually [39]. Cellulose consists of long chains of β-glucopyranose units linked by β-1,4-glycosidic bonds. Due to the abundance of -OH groups, it can be readily chemically modified through reactions with various reagents to enhance adsorption capacity [19].

The composition of algae depends on species, habitat, maturity, and environmental conditions. Ulva is a widely consumed green marine alga and is known for its rich content of nutrients, including polysaccharides, proteins, vitamins, and minerals, making it a popular edible seaweed worldwide [40]. The total dietary fiber content (both soluble and insoluble) in *Ulva lactuca* is slightly higher (54.9% of dry weight) than that in *Ulva pertusa* (52.1%). Analysis of the dietary fiber composition of *Ulva lactuca* shows that hemicellulose (20.6% of dry weight) is the most abundant component, followed by cellulose (9.1%) and lignin (1.5%). Among the monosaccharides, glucose (17.2% of dry weight) is the major constituent, followed by rhamnose (7.4%) and xylose (1.9%) [41].

In our previous studies, we reported the adsorption efficiency of different microalgae of varying particle sizes and compositions for Au(III), with or without lipid removal, using samples collected from different production batches [32,42]. The effective use of Ulva species for adsorptive recovery of rare earth metals has been reported in the literature [38]. However, to the best of our knowledge, no relevant studies have focused on their use as biosorbents for precious metal recovery. Therefore, this study aims to compare the Au(III) adsorption efficiency of two marine algae with different compositions, compare similarly treated microalgae, and ultimately to investigate the adsorption–reduction mechanism of cellulosic biomass. Practical limitations of raw adsorbents—such as slow adsorption rates, poor mechanical strength, low selectivity, difficulty in regeneration, and relatively low adsorption capacity—have been addressed through various chemical modification techniques, including esterification, graft polymerization, coating, and treatments with acids, alkalis, and methanol [3,37]. Improvements in the physical stability and adsorption capacity of chemically modified cellulose have been widely reported in the literature [19]. Among these methods, sulfuric acid treatment is a simple and cost-effective approach that enhances the chemical stability, selectivity, and mechanical strength of adsorbents. Potential environmental pollution during adsorbent preparation was minimized through a single-step treatment using non-volatile sulfuric acid. After preparation, the used sulfuric acid can be easily neutralized and safely discharged. This treatment improves adsorption efficiency by generating new adsorption sites through condensation of the polysaccharide matrix [15,43,44].

2. Experiment

2.1. Material and Analysis

For this study, the algae were provided by the Institute of Ocean Energy (IOES), Saga University, Japan. A stock solution of Au (25.0 mM; M = mol dm^{-3}) was prepared by dissolving the tetrachloroaurate complex ($HAuCl_4 \cdot 4H_2O$) and was subsequently diluted to desired concentrations for the experiments. All chemical reagents used in this study were of analytical grade, purchased from Wako Pure Chemical Industries Ltd., Osaka, Japan, and used without further purification. Test solutions for all experiments were prepared using deionized water, and the samples were stirred in a shaking incubator at controlled temperature.

The Fourier-transform infrared (FT-IR) spectra of all adsorbents before and after Au(III) adsorption were measured using an FT-IR spectrometer (Shimadzu, Affinity 1, Kyoto, Japan) with KBr pellets to identify functional group transformations during treatment and subsequent Au(III) adsorption. The concentrations of Au(III) ions in the test solutions before and after adsorption were determined using an inductively coupled plasma atomic emission spectrometer (ICP-AES; Shimadzu, ICPS-8100). Surface characterization of the adsorbents before and after Au(III) adsorption was carried out using a scanning electron microscope (SEM; Hitachi, SU-1500, Tokyo, Japan) and an energy-dispersive X-ray spectrometer (EDX; Hitachi, SU-8010). A digital microscope (Keyence, VHX-1000, Osaka, Japan)

was used to capture micrograph images of the adsorbents before and after Au adsorption. Additionally, X-ray diffraction (XRD) patterns of untreated and treated Au-loaded adsorbents were recorded using an X-ray diffractometer (Shimadzu, XRD-7000).

2.2. Preparation of Biosorbent

The treated adsorbents were prepared by agitating a mixture of 5.0 g of dry alga (*Ulva lactuca* or *Ulva pertusa*) with 50 cm^3 of concentrated sulfuric acid for 24 h at 373 K using a stirring speed of 220 rpm. After cooling, the mixture was neutralized with $NaHCO_3$ and repeatedly rinsed with distilled water until a neutral pH was achieved. The resulting black product was then dried for 24 h at 333 K in a convection oven. The dried material (1.10 g for *Ulva lactuca* and 1.35 g for *Ulva pertusa*) was subsequently ground to a particle size of 150 µm. The processed adsorbents were designed as treated *Ulva lactuca* (**TUL**) and treated *Ulva pertusa* (**TUP**). In addition, untreated adsorbents (expediently abbreviated as **DUL** and **DUP**) were prepared by directly grinding *Ulva lactuca* or *Ulva pertusa* to a particle size of 150 µm without any chemical treatment.

2.3. Biosorption Experiments

All experiments (except the kinetics study) were conducted at a temperature of 303 K and a shaking speed of 150 rpm. Time-dependent Au(III) adsorption experiments were carried out using a 2.0 mM Au(III) solution in 0.5 M HCl over a period of 0–120 h, and the effect of HCl concentration was investigated over the range of 0.01–2.0 M. The adsorption capacity was determined using metal solutions with concentrations ranging from 1.0 to 15.0 mM in 0.01 M HCl. Elution tests were performed only for treated adsorbents using various concentrations of acidic thiourea solution. At the end of each experiment, the mixture was filtered, and the metal ion concentrations in the filtrate, along with those in the initial solutions, were measured using ICP-AES. To minimize the consumption of the gold solution, single adsorption experiments were conducted; however, ICP-AES measurements were performed three times for each sample. The percentage adsorption, adsorption capacity, and percentage elution were calculated using Equations (1)–(3), respectively:

$$\% \text{ Adsorption} = \frac{C_i - C_e}{C_e} \times 100, \quad (1)$$

$$q = \frac{C_i - C_e}{W} \times V, \quad (2)$$

$$\% \text{ Elution} = \frac{C_{elu} - C_e}{C_i} \times 100, \quad (3)$$

where C_i [mol dm^{-3}] and C_e [mol dm^{-3}] are the initial and equilibrium concentrations, respectively. q represents the amount adsorbed [mol kg^{-1}], W is the dry weight of the adsorbent [kg], V is the volume of the test solution [dm^3], and C_{elu} is the concentration of eluted Au(III) [mol dm^{-3}].

3. Results and Discussion

3.1. Characterization of Adsorbents

Digital micrograph images captured before Au(III) adsorption for untreated and treated adsorbents are shown in Figure S1a–d. The greenish and fleshy forms of **DUL** and **DUP** changed to rigid black **TUL** and **TUP**, respectively, after treatment with concentrated sulfuric acid. FT-IR spectral data were used to analyze changes in functional groups in the algal biomass after sulfuric acid treatment and Au(III) adsorption. Figure S2a,b show absorption bands in the range of 3406–3414 cm^{-1}, corresponding to O–H stretching, and at 2922–2929 cm^{-1}, corresponding to C–H stretching vibrations. The absorption band at

1652 cm^{-1} for the untreated adsorbents represents the C=O of acid. After acid treatment, the biopolymer became more rigid, and water-soluble components were removed due to the breaking of some glycosidic linkages [45]. The peaks broadened, and the intensity of O–H stretching vibrations decreased, confirming that condensation had occurred. New peaks appeared at 1200–1215 cm^{-1} in **TUL** and **TUP**, attributed to C–O–C stretching vibrations, indicating condensation. The formation of ether linkages after treatment of polysaccharide-based biomass with sulfuric acid has also been reported in the literature [31,46,47]. An absorption peak around 1715 cm^{-1} corresponds to the C=O group of acid, likely resulting from the oxidation of primary hydroxyl groups. Sulfur trioxide, formed from concentrated sulfuric acid during heating, acts as an oxidizing reagent [42]. In Au-loaded adsorbents, peaks in the range of 3317–3390 cm^{-1} became broader due to interactions between hydroxyl groups and Au(III). The absorption peak at 1716 cm^{-1} also became sharper, likely due to the oxidation of some hydroxyl groups to carbonyl groups.

3.2. Effect of the Contact Time

The effect of contact time on the adsorption percentage of Au(III) onto **DUL**, **TUL**, **DUP**, and **TUP** is shown in Figure 1. The percentage of Au(III) adsorption increased with contact time, and equilibrium was reached after 72 h for **TUL** and 48 h for **TUP**, achieving 98% and 95% adsorption, respectively. Initially, the adsorption rate was higher because all adsorption sites on the adsorbents were vacant, allowing metal ions to easily diffuse onto the adsorbent surfaces. Subsequently, Au(III) ions penetrated the adsorbent surfaces, and after 72 h for **TUL** and 48 h for **TUP**, the ions fully occupied all available adsorption sites, resulting in a stable adsorption percentage. In contrast, the adsorption percentages for **DUL** and **DUP** were below 20% and were considered negligible.

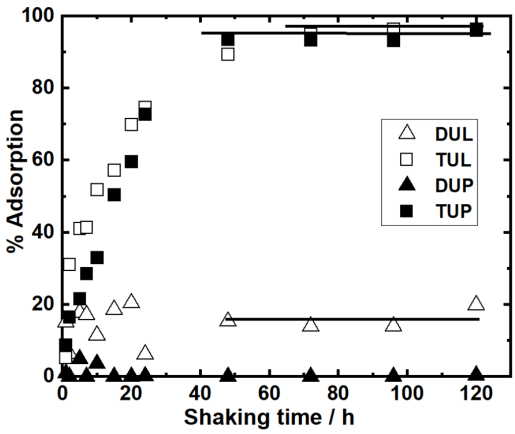

Figure 1. Effect of shaking time on percentage adsorption of Au(III) on **DUL**, **TUL**, **DUP**, and **TUP**. Weight of adsorbent = 10 mg, volume of solution = 10 cm^3, [Au(III)] = 2.0 mM, [HCl] = 0.50 M, shaking time = 0–120 h, shaking speed = 150 rpm, temperature = 303 K.

3.3. Effect of the HCl Concentration

Figure 2 shows the adsorption percentages of Au(III) on **DUL**, **TUL**, **DUP**, and **TUP** at various HCl concentrations (0.010 to 2.0 M). Although the untreated adsorbents exhibited low adsorption efficiencies—22% for **DUL** and 54% for **DUP** at 0.010 M HCl—the treated adsorbents demonstrated nearly quantitative adsorption of Au(III) across the entire range of HCl concentrations used in this study, with 96% and 100% adsorption on **TUL** and **TUP**, respectively. **DUL** and **DUP** partially dissolved at higher HCl concentrations, leading to material loss and reduced effectiveness. Consequently, their adsorption percentages decreased steadily with increasing HCl concentration. Even at a chloride ion concentration of 0.010 M, trivalent Au exists as the chloroaurate ion $AuCl_4^-$ but is still adsorbed as cationic

Au^{3+} on the adsorbent surface through coordination, forming cyclic complex compounds. Increasing the HCl concentration inhibits the adsorption of Au^{3+} by protonating ethereal oxygen groups and promoting the formation of $AuCl_4^-$.

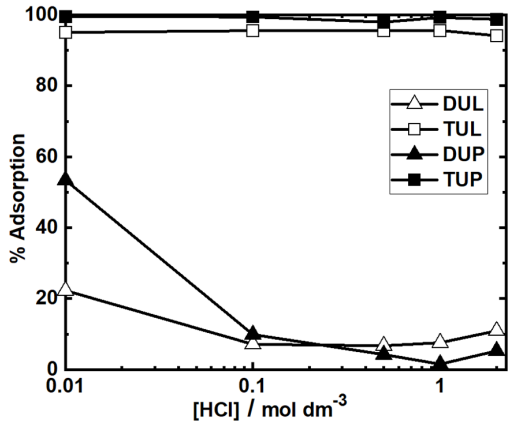

Figure 2. Effect of hydrochloric acid concentration on percentage adsorption of Au(III) on **DUL**, **TUL**, **DUP**, and **TUP**. Weight of adsorbent = 10 mg, volume of solution = 10 cm^3, [Au(III)] = 1.5 mM, [HCl] = 0.010–2.0 M, shaking time = 72 h, shaking speed = 150 rpm, temperature = 303 K.

Selectivity is a crucial factor when evaluating adsorption efficiency, especially in mixtures of coexisting metal ions. Figure 3a,b demonstrate the relationship between HCl concentration and the percentage of Au(III) adsorption in a competitive system on **TUL** and **TUP**, respectively. Both **TUL** and **TUP** exhibited outstanding selectivity and achieved quantitative adsorption of Au(III) from a mixture of PM ions in an acidic solution. Although increasing the HCl concentration appeared to suppress Au(III) adsorption, both **TUL** and **TUP** maintained satisfactory adsorption performance even at higher HCl concentrations. These findings highlight the strong potential of these materials for the selective adsorption of Au(III) from complex mixtures. The efficiency of the treated adsorbents in capturing Au(III) was not affected by the presence of other ions. The observed 32–35% adsorption of Pd(II) is likely due to the similarity in the tetrahedral geometry and coordination number between $PdCl_4^{2-}$ ions and $AuCl_4^-$ in an acidic chloride medium [17].

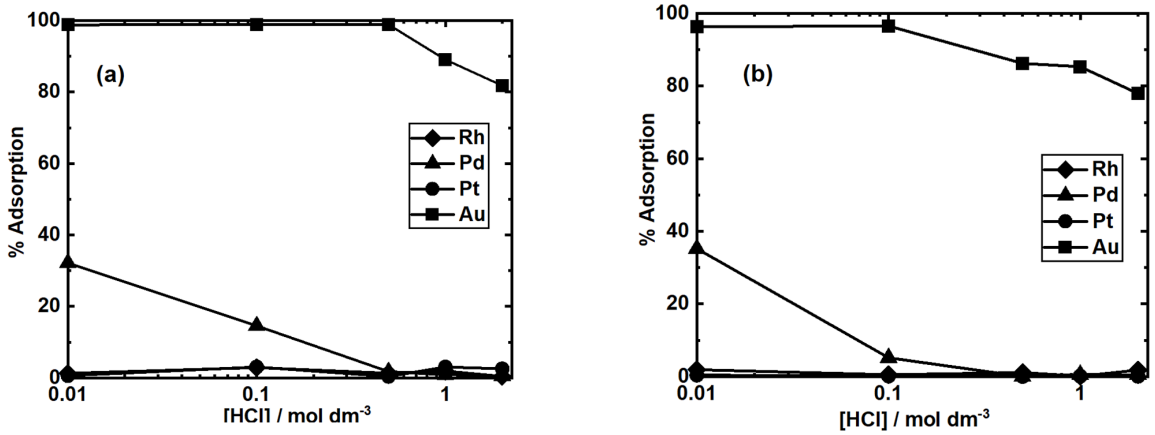

Figure 3. Effect of HCl concentration on the percentage adsorption of Au(III) in a competitive system on (**a**) **TUL** and (**b**) **TUP**. Weight of adsorbent = 10 mg, volume of solution = 10 cm^3, [PMs] each = 1.0 mM, [HCl] = 0.010–2.0 M, shaking time = 72 h, shaking speed = 150 rpm, temperature = 303 K.

The exceptional selectivity of treated algae for Au(III) adsorption is discussed in the subsequent section. However, because of the low adsorption efficiencies of **DUL** and **DUP**, no adsorption experiments using them were conducted in the competitive system.

3.4. Effect of the Equilibrium Metal Ion Concentration

The maximum Au(III) adsorption capacities of the untreated and treated adsorbents were evaluated using initial metal ion concentrations ranging from 1.0 to 15.0 mM. The adsorbed quantity initially increased with increasing Au(III) concentration and reached a plateau at higher concentrations, as shown in Figure 4a. The maximum adsorption capacities observed in the plateau region were 1.14, 6.57, 0.86, and 6.28 mol kg^{-1} for **DUL**, **TUL**, **DUP**, and **TUP**, respectively. Despite some variations in the chemical composition of the two algae species, the essential components responsible for Au(III) absorption were nearly identical. The equilibrium isotherm data were analyzed using the nonlinear Langmuir equation (Equation (4)) as well as the linearized form (Equation (5)) to verify the maximum loading capacity:

$$Q_e = \frac{bq_{max}C_e}{1 + bC_e}, \tag{4}$$

$$\frac{C_e}{Q_e} = \frac{1}{q_{max}\,b} + \frac{C_e}{q_{max}}, \tag{5}$$

where q_e is the equilibrium adsorption amount (mol kg^{-1}), q_{max} represents the maximum amount of metal ions adsorbed (mol kg^{-1}), and b represents the Langmuir constant related to the energy of adsorption (dm^3 mol^{-1}).

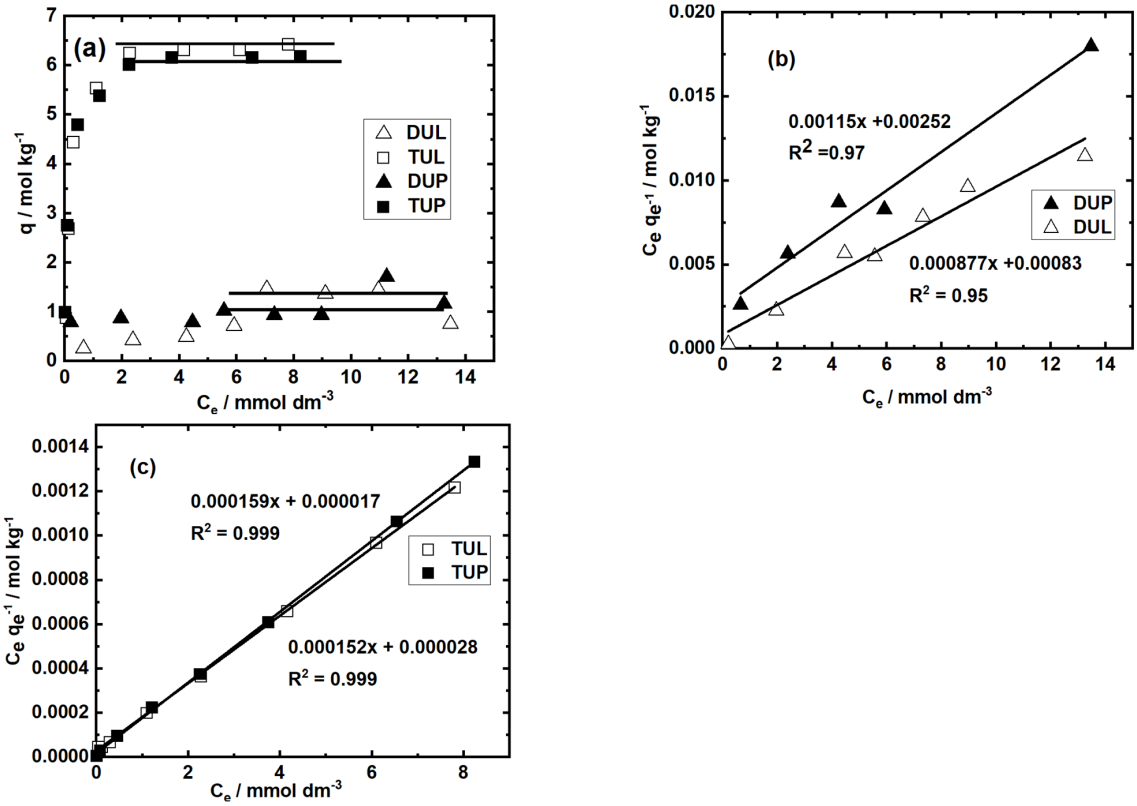

Figure 4. Effect of equilibrium Au(III) concentration on adsorbed amount of Au on (**a**) **DUL**, **TUL**, **DUP**, and **TUP**. (**b**) Langmuir plots of **DUL** and **DUP**. (**c**) Langmuir plot of **TUL** and **TUP**. Weight of adsorbent = 10 mg, volume of solution = 10 cm^3, [Au(III)] = 1.0–15.0 mM, [HCl] = 0.010 M, shaking time = 72 h, shaking speed = 150 rpm, temperature 303 K.

The maximum adsorption capacities, q_{max}, evaluated from the slopes of the Langmuir plots shown in Figure 4b,c, were in good agreement with the experimental values shown in Figure 4a. The high regression coefficient (R^2 = 0.999 for treated adsorbents and >0.95 for untreated adsorbents) indicate that the experimental data are well described by the

Langmuir adsorption isotherm, in which Au(III) ions form a monolayer on the adsorbent due to identical active sites [20]. The maximum loading capacities of **DUL**, **TUL**, **DUP**, and **TUP** are compared with those of various adsorbents reported in the literature in Table 1.

Table 1. Comparison of maximum loading capacities for Au(III) on various biosorbents.

Adsorbents	Maximum Loading Capacity mol kg^{-1}	References
Dithiocarbamate-modified cellulose	5.07	[3]
Sulfuric acid-treated lemon peel	6.5	[5]
Banana peel	2.1	[6]
Human hair	3.04	[11]
H_2SO_4-crosslinked Pinus patula bark	3.38	[15]
Poly(ethylene sulfide)-functionalized chitosan	3.33	[16]
Hydrothermally treated pomegranate peel	0.17	[20]
Proanthocyanidin-crosslinked sericin and alginate	1.2	[24]
Eggshell membrane	1.14	[27]
Glutaraldehyde-crosslinked chitosan	2.32	[28]
Sheep wool treated with Na_2S	0.95	[30]
Chicken feathers	0.7	[31]
Microalgae	3.25	[32]
Sulfuric acid-treated alginic acid	5.64	[47]
Sulfuric acid-crosslinked paper gel	5.05	[48]
Thioctic acid-modified Zr-MOF	1.76	[49]
Persimmon waste modified by DMA	5.63	[50]
Sulfuric acid-treated persimmon peel	4.5	[51]
Sulfuric acid-treated cotton cellulose	6.21	[52]
Ethylenediamine-modified wood lignin	3.08	[53]
DMA-modified wastepaper	4.6	[54]
Corn starch crosslinking with tannin acid	1.51	[55]
P aminobenzoic acid-modified wastepaper	5.1	[56]
Silk sericin	1	[57]
TUL	6.57	Present work
DUL	1.14	Present work
TUP	6.28	Present work
DUP	0.86	Present work

The maximum adsorption capacities of the treated adsorbents were higher than those of previously reported adsorbents. Additionally, thioctic acid-modified Zr-MOFs have been reported to possess a specific surface area with ultrahigh porosity for adsorption [48]; however, the loading capacities of **TUL** and **TUP** were found to be many times higher. Therefore, the results indicate that sulfuric acid treatment of algal biomass significantly improves adsorption capacity compared with treatments using other reagents [3,20,29,30]. This finding supports the feasibility of recovering Au(III) from industrial effluents using

these adsorbents. The higher adsorption capacities of **TUL** and **TUP** are attributed to the cleavage of glycosidic linkages during acid treatment. The parameters derived from the adsorption isotherms are listed in Table 2.

Table 2. Langmuir isotherm parameters for Au(III) on untreated and treated adsorbents.

Adsorbents	q_{max} (Observed)	q_{max} (Calculated)	b (dm^3 mol^{-1})	R^2
DUL	1.21	1.14	1056.8	0.950
DUP	1.16	0.88	461.4	0.970
TUL	6.51	6.57	5435.9	0.999
TUP	6.23	6.28	9366.4	0.999

3.5. Effect of the Adsorbent Dosage

The quantity of metal ions adsorbed from a liquid solution is significantly influenced by the amount of adsorbent used. A study was conducted to examine the effect of adsorbent dosage on adsorption by varying the solid-to-liquid ratio (S/L ratio) from 0.50 to 2.5 g dm^{-3} while keeping the concentration of Au(III) ions constant. The results are shown in Figure 5. As the amount of adsorbent increased, the efficiency of Au(III) adsorption sharply rose for **TUL** and **TUP**, reaching a plateau with over 95% adsorption at an S/L ratio of 1.0 g dm^{-3}. In contrast, the adsorption efficiency for **DUL** and **DUP** increased more gradually, reaching 25% and 90%, respectively, at an S/L ratio of 2.5 g dm^{-3}. This indicates that only a small amount of **TUL** or **TUP** is required to treat a large volume of Au(III) solution. As the quantity of adsorbent increased, the number of available binding sites for Au(III) ions also increased, leading to a plateau in the adsorption due to an excess of binding sites relative to the limited amount of adsorbate.

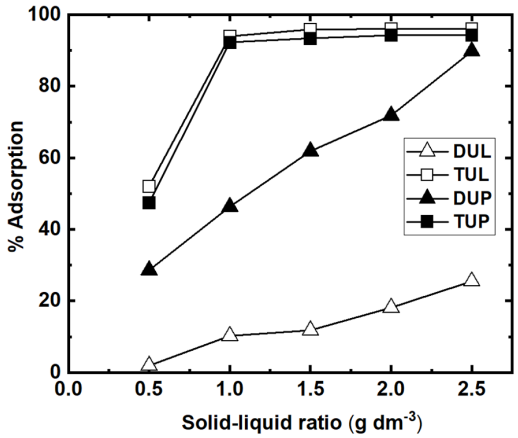

Figure 5. Effect of adsorbent dose on percentage adsorption of Au(III) on **DUL**, **TUL**, **DUP**, and **TUP**. Weight of adsorbent = 5.0–25 mg, volume of solution = 10 cm^3, [Au(III)] = 2.0 mM, [HCl] = 0.010 M, shaking time = 72 h, shaking speed = 150 rpm, temperature = 303 K.

3.6. Effect of Temperature

Studying kinetics is essential for evaluating the effectiveness of an adsorbent for adsorbing specific metal ions. This study examined the adsorption of Au(III) on **TUL** and **TUP** in 0.50 M HCl and temperatures of 293, 303, and 313 K, and the results are shown in Figure 6. The adsorption of Au(III) onto **TUL** and **TUP** was enhanced by increasing temperature, indicating that higher temperatures promote Au(III) uptake on the treated adsorbents. A similar effect of temperature on Au(III) adsorption has been reported for cellulose-based biomass [3]. The results showed that the pseudo-first-order model exhibited strong correlation coefficients (>0.96) for both types of algae. Based on the nonlinear

experimental plots, the adsorption efficiency increased with increasing temperature, and a contact time of 72 h was sufficient to reach equilibrium at 303 K. Furthermore, the time required to reach equilibrium decreased from 72 to 48 h for **TUL** and to 24 h for **TUP** when the temperature increased from 303 K to 313 K. However, equilibrium was not achieved within 72 h at 293 K. These findings indicate that increasing temperature can enhance otherwise slow adsorption kinetics.

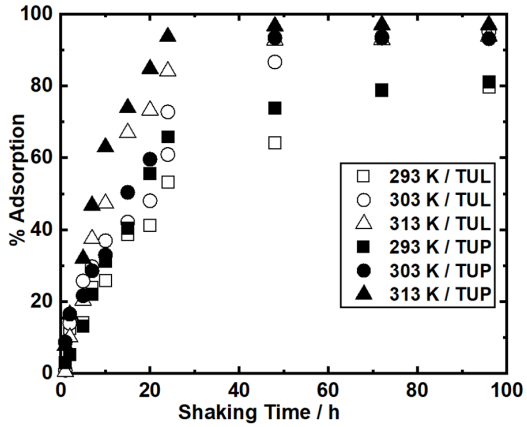

Figure 6. Effect of temperature on percentage adsorption of Au(III) on **TUL** and **TUP**. Weight of adsorbent = 10 mg, volume of solution = 10 cm^3, [Au(III)] = 2.0 mM, [HCl] = 0.50 M, shaking time = 0–96 h, shaking speed = 150 rpm, temperature = 293–313 K.

The initial rates of Au(III) adsorption on **TUL** and **TUP** were investigated using a pseudo-first-order kinetic model, described in Equation (6), at various temperatures:

$$\ln\frac{C_e}{C_i} = -\mathrm{kt}\,, \tag{6}$$

where k (h^{-1}) is the pseudo-first-order adsorption rate constant. By plotting $ln\ C_e/C_i$ versus t at three different temperatures, as shown in Figure 7a,b, all the plots exhibited linear relationships with correlation coefficients greater than 0.96.

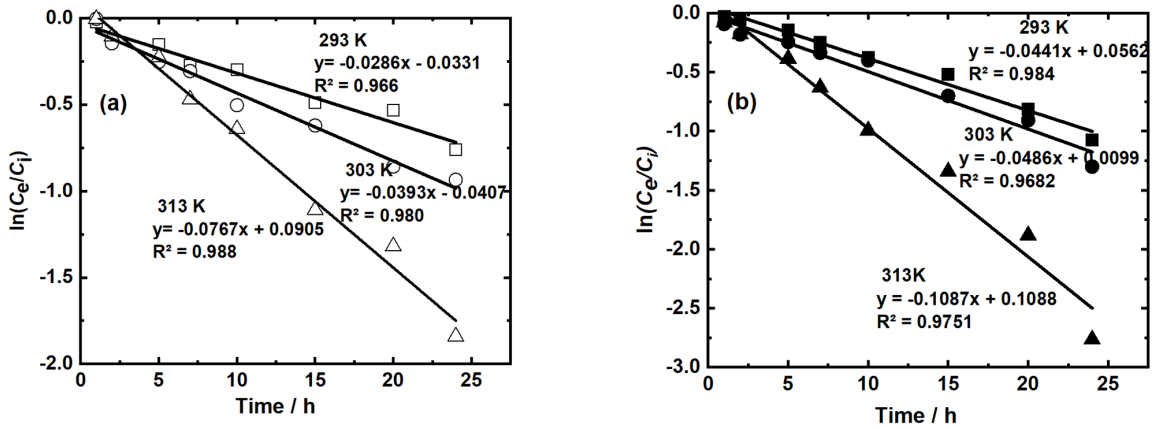

Figure 7. Pseudo-first order plot of Au(III) adsorption on (**a**) **TUL** and (**b**) **TUP**. Weight of adsorbent = 10 mg, volume of solution = 10 cm^3, [Au(III)] = 2.0 mM, [HCl] = 0.50 M, shaking speed = 150 rpm, shaking time = 0–24 h.

The pseudo-first-order rate constants were estimated from the slopes of these lines at different temperatures and are listed in Table 3. The values in Table 3 show that the reaction rate more than doubled when the temperature increased by 10 K from 303 to 313 K.

Table 3. Pseudo-first order constants and correlation coefficients for the adsorption of Au(III) on **TUP** and **TUL** at various temperatures.

Adsorbent	Temperature (K)	HCl (mol dm^{-3})	R^2	Rate Constant (h^{-1})
TUP	293	0.5	0.98	0.0441
	303	0.5	0.96	0.0486
	313	0.5	0.97	0.1087
TUL	293	0.5	0.96	0.0286
	303	0.5	0.98	0.0393
	313	0.5	0.98	0.0767

Activation energy is the minimum energy required for the chemical transformation of a compound. Its magnitude is crucial for determining the effect of temperature on the reaction rate and for distinguishing between physical and chemical adsorption processes. In physical adsorption, the forces involved are weak, and the activation energy is typically less than 5.0 kJ mol^{-1} [49,57,58]. In contrast, in chemisorption, the activation energy exceeds 8.2 kJ mol^{-1} due to stronger interactions [59]. The activation energy can be evaluated by plotting the pseudo-first-order rate constant at various temperatures using the Arrhenius equation, shown in Equation (7).

$$k_1 = \mathrm{A}\ \mathrm{e}^{-\mathrm{E_a}/\mathrm{RT}} \tag{7}$$

Equation (7) can be written as follows:

$$ln(k_1) = -\frac{E_a}{RT} + \ln(\mathrm{A}) \tag{8}$$

where k is the rate constant, E_a is the activation energy, T is the absolute temperature, and A, is the gas constant (8.314 J K^{-1} mol^{-1}). The plots of ln$k$ versus 1/T for the adsorption of Au(III) on **TUL** and **TUP** at various temperatures are shown in Figure 8.

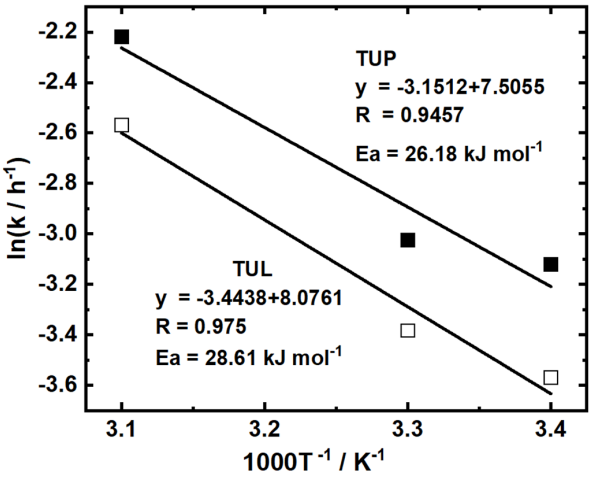

Figure 8. Arrhenius plot of Au(III) adsorption on **TUL** and **TUP**.

The apparent activation energies, E_a, for Au adsorption on **TUL** and **TUP** were estimated from the slopes of the linear plots, and the results are listed in Table 4. The positive E_a values suggest that the adsorption of Au(III) onto **TUL** and **TUP** is an endothermic chemical process. During Au adsorption, a gold-colored solid with a metallic appearance was observed. The relatively lower activation energy compared with other adsorbents reported in the literature is likely attributed to the reduction of Au(III) to Au(0) on the

adsorbent surface [57]. It has been reported that treatment using concentrated sulfuric acid reduces the E_a for Au uptake [43].

Table 4. Activation energy and correlation coefficient for adsorption of Au(III) on **TUP** and **TUL**.

Adsorbents	Activation Energy (*Ea*) kJ mol^{-1}	R^2 Value
TUL	26.18	0.94
TUP	28.61	0.97

3.7. Solid State Analysis

SEM/EDX, XRD, and digital photography were used to investigate the morphological changes in the adsorbents and the reduction of Au(III) to Au(0). Digital micrographs captured before and after treatment showed significant changes in surface morphology. The soft appearances of **DUL** and **DUP** (Figure S1a,c), became much tougher after treatment, as observed for **TUL** and **TUP** (Figure S1b,d), enabling them to better resist dissolution in concentrated HCl solution. Digital micrographs of Au-loaded **DUL**, **TUL**, **DUP**, and **TUP** show the presence of a bright gold-colored solid, as shown in Figure S3a–d. In addition, a thin layer of metallic particles floating on the surface of the HCl solution was observed for **TUL** and **TUP**, as shown in Figure S4. Although these particles gradually formed larger aggregates and settled at the bottom of the container, they remained distinct and separate from the adsorbent particles. Formation of a thin metallic layer has also been reported for various biomass-based adsorbents, such as persimmon peel [50], cotton cellulose [51], aminated wood lignin [52], and Kraft mill lignin [59].

Biomass-based adsorbents containing polyphenols [5,10,20,50] and polysaccharides [6,23,51] were found to be capable of converting adsorbed Au(III) to its metallic form. XRD patterns of the untreated and treated adsorbents are shown in Figure S5a,b. XRD patterns of Au-loaded **DUL**, **TUL**, **DUP**, and **TUP** confirmed the oxidation state of Au after adsorption. After chemical treatment, the untreated adsorbents no longer exhibited any crystallinity and instead showed a single broad peak at a 2θ value of approximately 23°. Cellulosic materials typically exhibited a peak at approximately 22.5° [39]. The Au-loaded untreated and treated adsorbents exhibited prominent diffraction peaks at 38.2°, 44.3°, 64.7°, and 77.6°. These face-centered cubic diffraction peaks indicate the reduction of ionic Au(III) to metallic Au(0). These peaks are consistent with those previously reported for metallic Au [5,6,47,50–52,60]. These findings indicate that abundant and inexpensive materials can be converted into high-value materials for Au recovery.

The SEM images of the crude and treated adsorbents prior to Au adsorption are shown in Figure S6. These images were used to examine morphological changes and to perform surface elemental analysis of all adsorbents. The treated algae exhibited a more rigid surface. Typical SEM images of **DUL** and **TUL**, as well as **DUP** and **TUP**, after Au(III) adsorption (Figure S7a and c, and Figure S8a and c, respectively) were used to identify and localize Au on the adsorbent surfaces. After adsorption, the Au-loaded adsorbents showed reduced porosities and more compact surface structures. Au particles appeared as clustered white spots distributed across the absorbent surface, suggesting that the adsorbed Au(III) ions were reduced to their elemental form. Moreover, no significant changes were observed in the surface morphologies of the adsorbents—especially the treated adsorbents—indicating that they remained intact during the adsorption, washing, and drying processes. The reduction of Au(III) to its metallic state was also confirmed by the appearance of microprecipitates in SEM images of brown algae [23] and dithiocarbamate-modified cellulose [3]. As expected, the EDX spectra of **DUL**, **TUL**, **DUP**, and **TUP** showed characteristic signals for their constituent elements. The appearance of new, high-intensity Au-related peaks in Figures S7b,d and S8b,d, without corresponding chlorine peaks, further

supports the reduction of Au(III) to its metallic state. The chlorine peak observed in **DUL** may be attributed to incomplete washing and was not detected in **TUL**, **DUP** or **TUP**. The peaks of C and O, along with other minor peaks, originated from the algae, and no nitrogen was detected.

3.8. Adsorption–Reduction of Au(III)

Biosorption mechanisms are predominantly based on electrostatic interactions between metal ions and surface functional groups [61]. Precious metals typically exist as anionic complexes, such as $AuCl_4^-$, $PtCl_6^{2-}$, $PdCl_4^{2-}$, and $RhCl_6^{3-}$, even at a chloride concentration of 0.010 M [52]. Under acidic conditions, surface functional groups become protonated and acquire positive charges. Electrostatic attraction is therefore expected to facilitate the interaction between negatively charged precious metal complexes and positively charged active sites on adsorbents. However, the adsorption rate shown in Figure 1 was remarkably slow, and the algae-based adsorbents did not exhibit affinity for other precious metals. If Au were adsorbed as $AuCl_4^-$, other precious metal anions would also be expected to adsorb with lower selectivity. Therefore, protonation (and the resulting electrostatic attraction) is unlikely to be the primary mechanism for Au adsorption. Instead, Au is proposed to be adsorbed in its cationic form, Au^{3+}, rather than as $AuCl_4^-$, via a coordination mechanism involving ethereal oxygen atoms. Previous studies have reported that the preferential adsorption of Au(III) is due to the higher reduction potential of $AuCl_4^-$ to Au(0) compared with those of other precious metals [3,40,47,52,57,59]. The present study supports the adsorption of Au in the Au^{3+} form, as illustrated in Scheme 1.

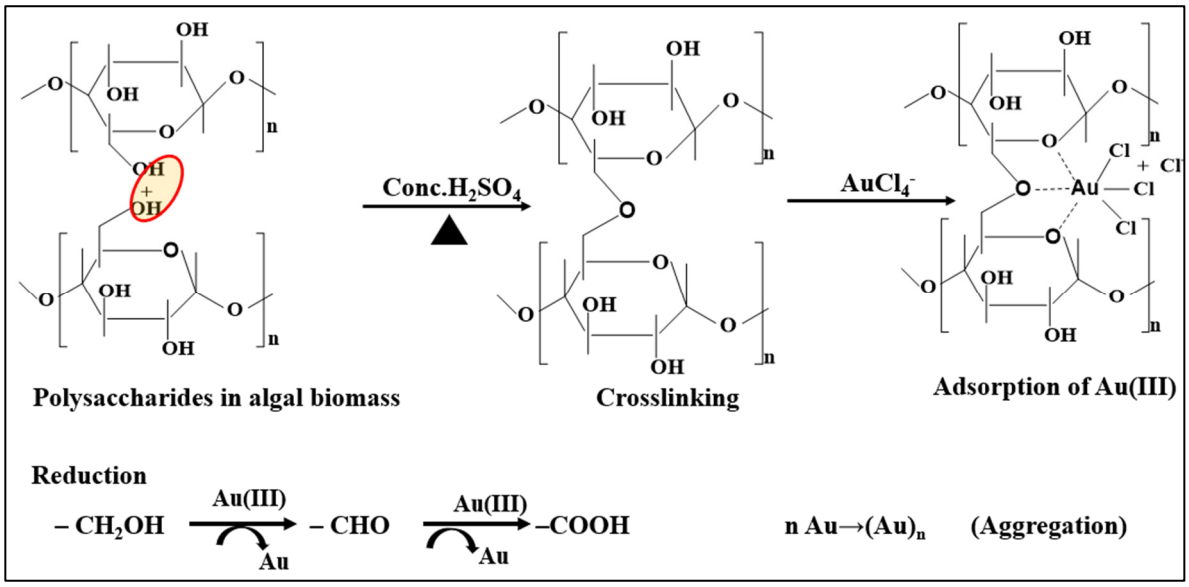

Scheme 1. Purposed mechanism of adsorption–reduction of Au(III) on algal biomass. Red circle was condensed to make ethereal linkage.

Algae contain various polysaccharides that can form new ethereal linkages (–C–O–C–) through condensation reactions with concentrated sulfuric acid, as supported by changes in the FT-IR spectra, including the appearance of a new absorption band at approximately 1195 cm^{-1}. The ethereal oxygen atom in the –C–O–C–bond, together with the pyranose oxygen atom, provides coordination sites for Au(III), enabling the formation of a five-membered ring structure. The adsorption of Au(III) occurs alongside its reduction to Au(0) by primary hydroxyl groups. It has been reported that the physicochemical properties and adsorption capacity of lemon peels improve after sulfuric acid treatment,

which also facilitates reduction to the elemental state [5]. Kuyucak and Volesky reported that algal cell walls are rich in polysaccharides containing hydroxyl groups; thus, the reduction of Au(III) to its metallic state is attributed to the oxidation of these hydroxyl groups to carbonyl groups [53]. The involvement of hydroxyl groups in the reduction of Au(III) to its elemental state has also been reported for brown algae [23], cross-linked paper gel [47], wastepaper [48], cotton cellulose [51], and Kraft mill lignin [59]. The role of hydroxyl groups in this reduction process is further supported by changes in the FT-IR spectra after adsorption. At higher Cl^- concentrations, protonation of ethereal oxygen atoms and the formation of $AuCl_4^-$ suppress the adsorption of Au^{3+}. Therefore, increasing the HCl concentration is less favorable for Au adsorption.

3.9. Adsorption–Desorption Study

Adsorption and desorption experiments were conducted to evaluate the potential for regeneration and reuse of the adsorbents, as well as the recovery of the adsorbed species. Desorption studies were carried out using various concentrations of acidic thiourea solution, and the results are shown in Figure 9.

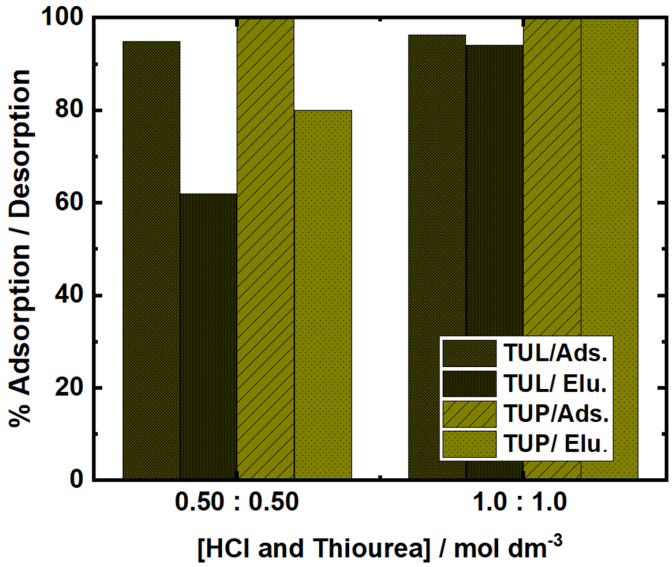

Figure 9. Adsorption and desorption profiles for **TUL** and **TUP**. Weight of adsorbent = 10 mg, volume of solution = 10 cm^3, [Au(III)] = 2.0 mM, [acidic thiourea] = 0.50–1.0 M, shaking time = 48 h, shaking speed = 150 rpm.

Although regeneration tests are important for the reuse of adsorbents, they were not included in this study because algae are available in sufficient quantities. Furthermore, due to their lower stability in strongly acidic environments, desorption experiments were not conducted for the untreated adsorbents. For **TUL** and **TUP**, 60% and 80% desorption were achieved, respectively, using 0.50 M acidic thiourea solution. Quantitative desorption of Au was increased when the concentration of acidic thiourea was increased to 1.0 M. During desorption, the increased chloride ion concentration from HCl displaced the Au(III) ions, followed by the formation of stable thiourea–Au complexes. Finally, the reduced Au was oxidized by thiourea, as shown in Equation (9). Acidic thiourea (1.0 M) effectively recovered the Au bound to the biomass and enabled its reuse in subsequent adsorption cycles.

$$Au^0 + 2(NH_2)_2SC \rightarrow Au[(NH_2)_2CS]_2^+ + e^-. \quad (9)$$

4. Conclusions

This study explored the effectiveness of two marine algae, *Ulva lactuca* and *Ulva pertusa*, in their crude state and after treatment using concentrated sulfuric acid for the adsorption of Au(III) in acidic chloride solutions. Although the crude adsorbents demonstrated acceptable performance, the treated adsorbents exhibited exceptional adsorption efficiencies and selectivity for Au(III). The adsorption kinetics of Au(III) followed a pseudo-first-order model, and the adsorption isotherms were well described by the Langmuir model. Treated adsorbents derived from the two marine algae showed maximum adsorption capacities of 6.57 and 6.28 mol kg^{-1}, respectively, representing a significant improvement over the raw adsorbents. Despite differences in composition, both species exhibited similar adsorption capacities due to the presence of comparable metal binding components. The adsorbed Au(III) ions were reduced to Au(0), contributing to an increase in the adsorption capacity. Increasing temperatures notably enhanced the adsorption capacities of **TUL** and **TUP** for gold ions. The adsorbed Au was efficiently recovered using an acidic thiourea solution. These results indicate that abundant and environmentally friendly algae have strong potential for industrial Au recovery. Overall, research on adsorption mechanisms and recovery processes of precious metals is valuable for advancing this field.

Supplementary Materials: The following supporting information can be downloaded at: https://www.mdpi.com/article/10.3390/separations13050137/s1, Figure S1: Digital micrograph images of (a) DUL, (b) TUL, (c) DUP, and (d) TUP before Au(III) adsorption; Figure S2: FT-IR spectra of (a) DUL and TUL, and (b) DUP, and TUP before and after Au(III) adsorption; Figure S3: Digital micrograph images of (a) DUL, (b) TUL, (c) DUP, and (d) TUP after Au(III) adsorption; Figure S4: Metallic flakes appeared in the equilibrium mixture of Au(III) solution using TUL used for adsorption isotherm experiment; Figure S5: XRD spectra of (a) DUL and TUL, and (b) DUP and TUP before and after Au(III) adsorption; Figure S6: SEM images of (a) DUL, (b) TUL, (c) DUP, and (d) TUP, before Au(III) adsorption; Figure S7: SEM images and EDX spectra of Au(III) loaded DUL and TUL. (a) DUL, (b) EDX spectra of DUL, (c) TUL, and (d) EDX spectra of TUL; Figure S8: SEM images and EDX spectra of Au(III) loaded DUP and TUP. (a) DUP, (b) EDX spectra of DUP, (c) TUP, and (d) EDX spectra of TUP.

Author Contributions: Conceptualization, K.O.; Methodology, G.P., S.M., H.K., K.O. and M.D.; Validation, G.P., S.M., K.O., M.D. and K.U.; Investigation, J.A.; Resources, M.D. and K.U.; Data curation, J.A. and K.O.; Writing—original draft, J.A.; Writing—review and editing, G.P. and K.O.; Visualization, H.K.; Supervision, K.O.; Project administration, K.O.; Funding acquisition, K.O. All authors have read and agreed to the published version of the manuscript.

Funding: This research received no external funding.

Data Availability Statement: The original contributions presented in this study are included in the article/Supplementary Material. Further inquiries can be directed to the corresponding author.

Acknowledgments: We are thankful to the Critical Metals Recovery subcommittee of the Co-creative Innovation platform for Renewable Energy (CIREn), Saga prefecture, Japan, for financial support to carry out this research. We are grateful to Tanaka Kikinzoku Kogyo K.K. (https://www.tanaka.co.jp/english/about/group/tkk.html (accessed on 26 April 2026)) for lending chloroauric acid solution. We are thankful to the Analytical Research Center for Experimental Sciences, Saga University, for SEM, EDX and XRD measurements.

Conflicts of Interest: The authors declare no conflicts of interest.

References

1. Sathishkumar, M.; Mahadevan, A.; Vijayaraghavan, K.; Pavagadhi, S.; Balasubramanian, R. Green recovery of gold through biosorption, biocrystallization, and pyro-crystallization. *Ind. Eng. Chem. Res.* **2010**, *49*, 7129–7135. [CrossRef]

2. Suzuki, S.; Iijima, H.; Kobayashi, Y.; Yamamoto, Y.; Shiigi, H.; Saitoh, N.; Konishi, Y. Biosorption of gold(III) from leachates of waste printed circuit boards by baker's yeast. *Hydrometallurgy* **2024**, *227*, 106323. [CrossRef]
3. Biswas, F.B.; Rahman, I.M.M.; Nakakubo, K.; Endo, M.; Nagai, K.; Mashio, A.S.; Taniguchi, T.; Nishimura, T.; Maeda, K.; Hasegawa, H. Highly selective and straightforward recovery of gold and platinum from acidic waste effluents using cellulose-based bio-adsorbent. *J. Hazard. Mater.* **2021**, *410*, 124569. [CrossRef] [PubMed]
4. Won, S.W.; Kotte, P.; Wei, W.; Lim, A.; Yun, Y.S. Biosorbents for recovery of precious metals review. *Bioresour. Technol.* **2014**, *160*, 203–212. [CrossRef]
5. Parajuli, D.; Kawakita, H.; Kajiyama, K.; Ohto, K.; Harada, H.; Inoue, K. Recovery of gold from hydrochloric acid by using lemon peel gel. *Sep. Sci. Technol.* **2008**, *43*, 2363–2374. [CrossRef]
6. Bediako, J.K.; Choi, J.W.; Song, M.H.; Zhao, Y.; Lin, S.; Sarkar, A.K.; Cho, C.W.; Yun, Y.S. Recovery of gold via adsorption-incineration techniques using banana peel and its derivatives: Selectivity and mechanisms. *Waste Manag.* **2020**, *113*, 225–235. [CrossRef]
7. Sharma, R.; Suhendra, N.F.; Jung, S.H.; Lee, H. Gold recovery at ultra-high purity from electronic waste using selective polymeric film. *Chem. Eng. J.* **2023**, *451*, 138506. [CrossRef]
8. Ghomi, A.G.; Kolur, N.A.; Sharifian, S.; Golnaraghi, A. Biosorption for sustainable recovery of precious metals from wastewater. *J. Environ. Chem. Eng.* **2020**, *8*, 103996. [CrossRef]
9. Park, I.-S.; Kwak, I.S.; Bae, M.A.; Mao, J.; Won, S.W.; Han, D.H.; Chung, Y.S.; Yun, Y.S. Recovery of gold as a type of porous fiber by using biosorption followed by incineration. *Bioresour. Technol.* **2012**, *104*, 208–214. [CrossRef]
10. Ortinero, C.V.; Meim, H.N.; Paragas, D.S. Biosorbents from Mangifera indica l. peel for the recovery of gold from electronic waste. *J. Ecol. Eng.* **2022**, *23*, 102–108. [CrossRef]
11. Yu, D.; Morisada, S.; Kawakita, H.; Sakaguchi, K.; Osada, S.; Ohto, K.; Inoue, K.; Song, X.; Zhang, G.; Sathuluri, R.R. Gold recovery from precious metals in acidic media by using human hair waste as a new pretreatment-free green material. *J. Environ. Chem. Eng.* **2021**, *9*, 104724. [CrossRef]
12. Forti, V.; Balde, C.P.; Kuehr, R.; Bel, G. *The Global e-Waste Monitors 2020: Quantities, Flows and the Circular Economy Potential*; United Nations University (UNU)/United Nations Institute for Training and Research (UNITAR)–Co-Hosted SCYCLE Programme, International Telecommunication Union (ITU) & International Solid Waste Association (ISWA): Bonn, Germany; Geneva, Switzerland; Rotterdam, The Netherlands, 2020.
13. Li, F.; Zhu, J.; Sun, P.; Zhang, M.; Li, Z.; Xu, D.; Gong, X.; Zou, X.; Geim, A.K.; Su, Y.; et al. Highly efficient and selective extraction of gold by reduced graphene oxide. *Nat. Commun.* **2022**, *13*, 4472. [CrossRef]
14. Adeeyo, A.O.; Bello, O.S.; Agboola, O.S.; Adeeyo, R.O.; Oyetade, J.A.; Alabi, M.A.; Edokpayi, J.N.; Makungo, R. Recovery of precious metals from processed wastewater: Conventional techniques nexus advanced and pragmatic alternatives. *Water Reuse* **2023**, *13*, 134–161. [CrossRef]
15. Petins, M.M.C.; Villa, R.A.S.; Benítez, R.B.; Corredor, J.C.A. Chemical modified tannins from Pinus patula bark for selective biosorption of gold in aqueous media. *J. Environ. Chem. Eng.* **2021**, *9*, 106162. [CrossRef]
16. Wang, S.; Wang, H.; Wang, S.; Zhang, L.; Fu, L. Highly effective and selective adsorption of Au(III) from aqueous solution by poly(ethylene sulfide) functionalized chitosan: Kinetics, isothermal adsorption and thermodynamics. *Microporous Mesoporous Matel.* **2022**, *341*, 112074. [CrossRef]
17. Mack, C.; Wilhelmi, B.; Duncan, J.R.; Burgess, J.E. Biosorption of precious metals: Research review paper. *Biotechnol. Adv.* **2007**, *25*, 264–271. [CrossRef]
18. Guo, J.; Wu, Y.; Wang, Z.; Yu, J.; Li, J.R. Adsorbents for the recovery of precious metals from wastewater. *J. Mater. Sci.* **2022**, *57*, 10886–10911. [CrossRef]
19. Hokkanen, S.; Bhatnagar, A.; Sillanpää, M. A review on modification methods to cellulose based adsorbents to improve adsorption capacity. *Water Res.* **2016**, *91*, 156–173. [CrossRef] [PubMed]
20. Zhu, Q.; Zhu, J.; Huang, K. Selectivity of modified pomegranate peel for gold, platinum, and palladium: Adsorption behavior, mechanism, and recovery. *J. Environ. Chem. Eng.* **2024**, *12*, 11190. [CrossRef]
21. Eisler, R. Biorecovery of gold. *Indian J. Exp. Biol.* **2003**, *41*, 967–971. Available online: https://nopr.niscpr.res.in/handle/123456789/17160 (accessed on 26 April 2026). [PubMed]
22. Inoue, K.; Gurung, M.; Xiong, Y.; Kawakita, H.; Ohto, K.; Alam, S. Hydrometallurgical recovery of precious metals and removal of hazardous metals using persimmon tannin and persimmon wastes. *Metals* **2015**, *5*, 1921–1956. [CrossRef]
23. Mata, Y.N.; Torres, E.; Blázquez, M.L.; Ballester, A.; González, F.; Muñoz, J.A. Gold(III) biosorption and bioreduction with the brown alga Fucus vesiculosus. *J. Hazard. Mater.* **2009**, *166*, 612–618. [CrossRef] [PubMed]
24. Santos, N.T.G.; Moraes, L.F.; Silva, M.G.C.; Vieira, M.G.A. Recovery of gold through adsorption onto sericin and alginate particles chemically crosslinked by proanthocyanidins. *J. Clean. Prod.* **2020**, *253*, 119925. [CrossRef]
25. Vijayaraghavan, K.; Mahadevan, A.; Sathishkumar, M.; Pavagadhi, S.; Balasubramanian, R. Biosynthesis of Au(0) from Au(III) via biosorption and bioreduction using brown marine alga Turbinaria conoides. *Chem. Eng. J.* **2011**, *167*, 223–227. [CrossRef]

26. Znad, H.; Awual, M.-R.; Martini, S. The utilization of algae and seaweed biomass for bioremediation of heavy metal-contaminated wastewater. *Molecules* **2022**, *27*, 1275. [CrossRef]
27. Ishikawa, S.; Suyama, K.; Arihara, K.; Itoh, M. Uptake and recovery of gold ions from electroplating wastes using eggshell membrane. *Bioresour. Technol.* **2002**, *81*, 201–206. [CrossRef]
28. Aktas, S.; Gozuak, B.; Acma, H.; Ozalp, M.R.; Acma, E. Gold recovery from chloride solutions using fallen leaves. *Environ. Chem. Lett.* **2011**, *9*, 47–53. [CrossRef]
29. Enkhzaya, S.; Shiomori, K.; Oyuntsetseg, B. Effective adsorption of Au(III) and Cu(II) by chemically treated sheep wool and the binding mechanism. *J. Environ. Chem. Eng.* **2020**, *8*, 104021. [CrossRef]
30. Suyama, K.; Fukazawa, Y.; Suzumura, H. Biosorption of precious metal ions by chicken feather. *Appl. Biochem. Biotechnol.* **1996**, *57*, 67–74. [CrossRef]
31. Khunathai, K.; Xiong, Y.; Biswas, B.K.; Adhikari, B.B.; Kawakita, H.; Ohto, K.; Inoue, K.; Kato, H.; Kurata, M.; Atsumi, K. Selective recovery of gold by simultaneous adsorption–reduction using microalgal residues generated from biofuel conversion processes. *J. Chem. Technol. Biotechnol.* **2012**, *87*, 393–401. [CrossRef]
32. Adhikari, J.; Pang, G.; Morisada, S.; Kawakita, H.; Ohto, K.; Inoue, K.; Demura, M.; Meada, S.; Nakamizo, K. Defatted microalgae Haematococcus pluvialis: A sustainable source for gold recovery. *J. Environ. Chem. Eng.* **2024**, *12*, 113804. [CrossRef]
33. Schiewer, S.; Volesky, B. Biosorption by marine algae. In *Bioremediation*; Springer: Dordrecht, The Netherland, 2000; pp. 139–169. [CrossRef]
34. Dong, Z.; Liu, J.; Yuan, W.; Yi, Y.; Zhao, L. Recovery of Au(III) by radiation synthesized aminomethyl pyridine functionalized adsorbents based on cellulose. *Chem. Eng. J.* **2016**, *283*, 504–513. [CrossRef]
35. Soundararajan, R.K.V.; Varjani, S.; Chandrasekaran, R.; Kandasamy, D. Chap. 17 Recovery of gold and other precious metals by biosorption. In *Sustainable Resource Management, Volume I: Technologies for Recovery and Reuse of Energy and Waste Materials*; Guo, W., Ngo, H.-H., Surampalli, R.Y., Zhang, T.C., Eds.; John Wiley & Sons: Hoboken, NJ, USA, 2021; pp. 464–488. [CrossRef]
36. Areco, M.M.; Hanel, S.; Duran, J.; Afonso, M.S. Biosorption of Cu(II), Zn(II), Cd(II) and Pb(II) by dead biomasses of green alga *Ulva lactuca* and the development of a sustainable matrix for adsorption implementation. *J. Hazard. Mater.* **2012**, *214*, 123–132. [CrossRef]
37. Torres, E. Biosorption: A review of the Latest Advances. *Processes* **2020**, *8*, 1584. [CrossRef]
38. Manikandan, N.A.; Lens, P.N.L. Biorefining of green macroalgal (*Ulva* sp.) biomass and its application in the adsorptive recovery of rare earth elements (REEs). *Sep. Purif. Technol.* **2022**, *303*, 122200. [CrossRef]
39. Suhas; Gupta, V.K.; Carrott, P.J.M.; Singh, R.; Chaudhary, M.; Kushwaha, S. Cellulose: A review as natural, modified and activated carbon adsorbent. *Bioresour. Technol.* **2016**, *216*, 1066–1076. [CrossRef]
40. Wahlstrom, N.; Edlund, U.; Pavia, H.; Toth, G.; Jaworski, A.; Pell, A.J.; Choong, F.X.; Shirani, H.; Nilsson, K.P.R.; Dahlfors, A.R. Cellulose from the green macroalgae *Ulva lactuca*: Isolation, characterization, optotracing, and production of cellulose nanofibrils. *Cellulose* **2020**, *27*, 3707–3725. [CrossRef]
41. Yaich, H.; Garna, H.; Besbes, S.; Paquot, M.; Blecker, C.; Attia, H. Chemical composition and functional properties of *Ulva lactuca* seaweed collected in Tunisia. *Food Chem.* **2011**, *128*, 895–901. [CrossRef]
42. Adhikari, J.; Sakamura, R.; Kawakita, H.; Morisada, S.; Ohto, K.; Inoue, K.; Demura, M. Au(III) recovery using two microalgal adsorbents with or without treatment with concentrated sulfuric acid. *J. Water Process Eng.* **2023**, *56*, 104520. [CrossRef]
43. Chang, S.H. Gold (III) recovery from aqueous solutions by raw and modified chitosan: A review. *Carbohydr. Polym.* **2021**, *256*, 117423. [CrossRef]
44. Gurung, M.; Adhikari, B.B.; Kawakita, H.; Ohto, K.; Inoue, K.; Alam, S. Recovery of Au(III) by using low-cost adsorbent prepared from persimmon tannin extract. *Chem. Eng. J.* **2011**, *174*, 556–563. [CrossRef]
45. Gurung, M.; Adhikari, B.B.; Gao, X.; Alam, S.; Inoue, K. Sustainability in the metallurgical industry: Chemically modified cellulose for selective biosorption of gold from mixtures of base metals in chloride media. *Ind. Eng. Chem. Res.* **2014**, *53*, 8565–8576. [CrossRef]
46. Pangeni, B.; Paudyal, H.; Abe, M.; Inoue, K.; Kawakita, H.; Ohto, K.; Adhikari, B.B.; Alam, S. Selective recovery of gold using some cross-linked polysaccharide gels. *Green Chem.* **2012**, *14*, 1917–1927. [CrossRef]
47. Pangeni, B.; Paudyal, H.; Inoue, K.; Kawakita, H.; Ohto, K.; Alam, S. An assessment of gold recovery processes using cross-linked paper gel. *J. Chem. Eng. Data* **2012**, *57*, 796–804. [CrossRef]
48. Wang, C.; Lin, G.; Zhao, J.; Wang, S.; Zhang, L.; Xi, Y.; Li, X.; Ying, Y. Highly selective recovery of Au(III) from wastewater by Thioctic acid modified Zr-MOF: Experiment and DFT calculation. *Chem. Eng. J.* **2020**, *380*, 122511. [CrossRef]
49. Xiong, Y.; Adhikari, C.R.; Kawakita, H.; Ohto, K.; Inoue, K.; Harada, H. Selective recovery of precious metals by persimmon waste chemically modified with dimethylamine. *Bioresour. Technol.* **2009**, *100*, 4083–4089. [CrossRef]
50. Parajuli, D.; Kawakita, H.; Inoue, K.; Ohto, K.; Kajiyama, K. Persimmon peel gel for the selective recovery of gold. *Hydrometallurgy* **2007**, *87*, 133–139. [CrossRef]

51. Pangeni, D.; Paudyal, H.; Inoue, K.; Kawakita, H.; Ohto, K.; Alam, S. Selective recovery of gold(III) using cotton cellulose treated with concentrated sulfuric acid. *Cellulose* **2012**, *19*, 381–391. [CrossRef]
52. Parajuli, D.; Kawakita, H.; Inoue, K.; Funaoka, M. Recovery of gold(II), palladium(II), and platinum(IV) by aminated lignin derivative. *Ind. Eng. Chem. Res.* **2006**, *45*, 6405–6412. [CrossRef]
53. Adhikari, C.R.; Parajuli, D.; Kawakita, H.; Inoue, K.; Ohto, K.; Harada, H. Dimethylamine-modified wastepaper for the recovery of precious metals. *Environ. Sci. Technol.* **2008**, *42*, 5486–5491. [CrossRef]
54. Liu, F.; Peng, G.; Li, T.; Yu, G.; Deng, S. Au(III) adsorption and reduction to gold particles on cost-effective tannin acid immobilized dialdehyde corn starch. *Chem. Eng. J.* **2019**, *3702*, 228–236. [CrossRef]
55. Adhikari, C.R.; Parajuli, D.; Inoue, K.; Ohto, K.; Kawakita, H.; Harada, H. Recovery of precious metals by using chemically modified wastepaper. *New J. Chem.* **2008**, *32*, 1634–1641. [CrossRef]
56. Chen, X.; Lam, K.F.; Mak, S.F.; Yeung, K.L. Precious metal recovery by selective adsorption using biosorbents. *J. Hazard. Mater.* **2011**, *186*, 902–910. [CrossRef] [PubMed]
57. Parajuli, D.; Adhikari, C.R.; Kawakita, H.; Yamada, S.; Ohto, K.; Inoue, K. Chestnut pellicle for the recovery of gold. *Bioresour. Technol.* **2009**, *100*, 1000–1002. [CrossRef]
58. Unuabonah, E.I.; Adebowale, K.O.; Olu-Owolabi, B.I. Kinetic and thermodynamic studies of the adsorption of lead (II) ions onto phosphate-modified kaolinite clay. *J. Hazard. Mater.* **2007**, *144*, 386–395. [CrossRef]
59. Adhikari, B.B.; Gurung, M.; Alam, S.; Tolnai, B.; Inoue, K. Kraft mill lignin–a potential source of bio-adsorbents for gold recovery from acidic chloride solution. *Chem. Eng. J.* **2013**, *231*, 190–197. [CrossRef]
60. Das, N. Recovery of precious metals through biosorption: A review. *Hydrometallurgy* **2010**, *103*, 180–189. [CrossRef]
61. Puvvada, G.V.A.; Sridhar, R.; Lakshmanan, V.I. Chloride metallurgy: PGM recovery and titanium dioxide production. *JOM* **2003**, *55*, 38–41. [CrossRef]